

## Next Generation Sequencing And Drug Repositioning Approach For Motor Neuron Disease

Uma Kumari<sup>1</sup> Nathan Jose Kumar C<sup>1</sup> Krishnalaya Ramakrishnan<sup>2</sup> Gokulan S.S<sup>2</sup> Roma Sharma<sup>3</sup> Kamal Hasan<sup>3</sup>

<sup>1</sup>Senior Bioinformatics Scientist, Bioinformatics Project and Research Insitute, Noida - 201301, India

<sup>1</sup>Project Trainee at Bioinformatics Project and Research Insitute, Noida - 201301, India

<sup>2</sup>Project Trainee at Bioinformatics Project and Research Insitute, Noida - 201301, India

<sup>2</sup>Project Trainee at Bioinformatics Project and Research Insitute, Noida - 201301, India

<sup>3</sup>Project Trainee at Bioinformatics Project and Research Insitute, Noida - 201301, India

<sup>3</sup>Project Scientist ICMR NIIH, Mumbai, India

### Abstract

This investigation employs a multidimensional methodology to explore the intricacies of motor neuron disease (MND), with a specific emphasis on amyotrophic lateral sclerosis (ALS) associated with the mutant SOD1 gene. Through a synthesis of structural examination, computational simulations, and genetic profiling, the study endeavors to elucidate pivotal facets of MND pathology and discern prospective therapeutic interventions. Leveraging sophisticated structural visualization platforms such as Rasmol and PyMOL, the research scrutinizes the intricate three-dimensional framework of the mutant SOD1 protein (PDB ID: 1UXL), elucidating its significance in the progression of the disease. Next-generation sequencing, augmented by sequence homology and phylogenetic analyses, elucidates the genetic foundations of ALS-related MND, furnishing essential insights into disease causation. Molecular docking simulations utilizing CurPocket unveil distinct binding attributes of potential therapeutics, including Riluzole and Gabapentin, within specific loci of the mutant SOD1 protein. Validation via ERRAT, SAVES, and Ramachandran plot analysis confirms the structural robustness of the protein model, reinforcing the reliability of the findings. This integrative approach engenders a comprehensive comprehension of mutant SOD1 in MND, providing valuable perspectives into potential therapeutic avenues for alleviating the debilitating ramifications of this neurodegenerative affliction. By amalgamating structural biology, computational modeling, and genomic scrutiny, this study enriches the evolving corpus of knowledge endeavoring to propel MND research forward and expedite the emergence of tailored therapeutic modalities.

**Keywords:** Motor Neuron Disease; amyotrophic lateral sclerosis; Structure Validation ;Homology Modeling, Molecular Docking ,Next-Generation Sequencing.

### Introduction

Motor neuron diseases (MNDs) represent a spectrum of progressive neurological disorders characterized by the deterioration of motor neurons essential for vital voluntary muscle functions, including speech, locomotion, respiration, swallowing, and overall bodily movement [1]. These conditions progressively compromise the nervous system's capacity to regulate voluntary muscle activity, resulting in a myriad of challenges that impede essential daily functions [2]. The pathophysiology of MND involves dysfunction of either the upper motor neurons located in the precentralgyrus of the frontal lobe or the lower motor neurons situated in the ventral horn of the spinal cord, typically culminating in weakness devoid of discernible sensory symptoms or pain [3]. MNDs can manifest as either hereditary or acquired conditions, exhibiting variations in underlying pathology and clinical presentations [4]. The categorization of MNDs encompasses five distinct groups based on inheritance patterns, clinical manifestations, and the site of motor neuron degeneration, which include Amyotrophic lateral sclerosis (ALS), primary lateral sclerosis (PLS), progressive muscular atrophy (PMA), progressive bulbar palsy (PBP), and pseudobulbar palsy [5]. Among these, amyotrophic lateral sclerosis, also known as Lou Gehrig's disease or Charcot disease, stands as the most prevalent form of motor neuron degeneration in adults, typically peaking in onset during the sixth or seventh decades of life [6]. Patients commonly experience a gradual onset of motor weakness, initially localized and subsequently spreading throughout the body, leading to paralysis and eventual mortality within a few years of diagnosis [7]. Although ALS predominantly manifests sporadically, approximately 10% of cases exhibit a familial component (fALS), with about 20% of familial cases associated with mutations in the superoxide dismutase 1 (SOD1) gene [8]. Superoxide dismutase 1 (SOD1) plays a crucial role as an antioxidant enzyme, pivotal in protecting cells against the deleterious effects of superoxide radicals [9]. Its mechanism involves the binding of copper and zinc ions, essential for directly deactivating toxic superoxide radicals [10]. Mutations within the SOD1 gene can lead to both gain-of-function and loss-of-function alterations, thereby impacting its enzymatic activity and cellular protective functions [11]. The integration of Next-Generation Sequencing (NGS) with drug repositioning

strategies represents an innovative approach in drug discovery, particularly for complex diseases like MND. NGS, with its high-throughput genomic profiling capabilities, enables researchers to comprehensively analyze the genetic landscape of diseases and identify key genetic factors and molecular pathways [12]. When combined with drug repositioning, this genomic information becomes a powerful tool for discovering potential therapeutic interventions [13]. In the pursuit of alternative and more effective therapies, a promising strategy involves drug repurposing, aiming to identify new applications for medications beyond their original indications, utilizing drugs already approved by regulatory agencies such as the US Food and Drug Administration (FDA). Riluzole stands as the sole neuroprotective compound endorsed by the FDA for clinical use in treating ALS/MND. Its neuroprotective effects are believed to stem from its actions on presynaptic and postsynaptic pathways involved in regulating glutamatergic neurotransmission, rendering it effective as an antiglutamate agent [14]. The pharmacological effects of Riluzole derive from its various mechanisms of action, including decreasing the frequency of repetitive firing, inhibiting persistent sodium currents in motoneurons, enhancing calcium-dependent potassium currents, reducing neurotransmitter release at presynaptic sites, and attenuating responses of neurotransmitter receptors at postsynaptic sites [15]. Due to its diverse mechanisms of action, Riluzole finds utility in the treatment of various neurological disorders beyond ALS, including Parkinson's disease, Huntington's disease, Machado-Joseph's disease, multiple sclerosis, spinal muscular atrophy, as well as anxiety, autism, depression, and schizophrenia disorders [16]. Gabapentin (GBP) is a structural derivative of the neurotransmitter gamma-aminobutyric acid (GABA). While its precise mechanism of action remains uncertain, it is known to influence the gamma-aminobutyric acid and glutamate neurotransmitter systems by inhibiting glutamate synthesis and promoting its degradation [17]. Pharmacological agents enhancing GABAergic activity, such as gabapentin, represent potential therapeutic interventions for ALS [18]. This study aims to utilize next-generation sequencing and drug repositioning strategies for the mutant form of the human SOD1 gene. Riluzole and gabapentin emerge as promising candidates for drug repurposing due to their significant binding affinity with the protein 1UXL. The study employs a diverse array of methodologies encompassing structural analysis, sequence similarity assessment, and molecular docking simulations. The utilization of sophisticated tools such as RasMol, PyMOL, BLAST, COBAL, and CurPocket facilitates comprehensive exploration and evaluation of protein structure and potential therapeutic interactions. The validation of protein structural integrity via ERRAT and SAVES enhances the credibility of findings, thereby providing deeper insights into the role of mutant SOD1 in MND and offering promising avenues for therapeutic intervention [19,20].

## Material And Methods

The computational analysis in this study commenced with the retrieval of target information from the National Center for Biotechnology Information (NCBI) database, including the unique Protein Data Bank (PDB) identifier (PDB ID: 1UXL). Subsequently, the three-dimensional structure corresponding to the target protein was acquired in PDB format from the Protein Data Bank (PDB) repository [21,22]. RasMol software was employed for the visualization and analysis of hydrogen bonding patterns within the protein structure. This visualization facilitated the identification of a complex network of hydrogen bonds, emphasizing the pivotal residues involved in stabilizing the tertiary structure of the protein. Leveraging color-coded representation in RasMol enabled a clear differentiation between various types of hydrogen bonds, thereby providing a comprehensive overview of the bonding architecture. Visualization of protein structures serves as a fundamental tool for enhancing researchers' understanding of protein three-dimensional (3D) architecture, which is essential for elucidating protein function, interactions, and mechanisms. Particularly in the field of drug discovery, protein structure visualization plays a critical role in aiding researchers to identify potential drug-binding sites, anticipate ligand-protein interactions, and devise innovative drug candidates, thus facilitating rational drug design processes [23,24]. Sequence similarity analysis conducted through Basic Local Alignment Search Tool (BLAST) revealed significant matches for the query sequence against known sequences. The target protein was identified as a member of the superoxide dismutase family protein, characterized by a specific domain architecture (ID: 10085118) [25,26]. The visualization of the protein surface using PyMOL software allowed for a detailed examination of its spatial arrangement, enabling the identification of potential functional sites, interactions, and structural features, thereby contributing to a deeper comprehension of the protein's molecular biology. Volume rendering visualization, a technique utilized in computer graphics and medical imaging, was employed to represent the three-dimensional data sets of the protein structure. Visualizing the active site residues in PyMOL in stick form facilitated a detailed inspection of the atomic structure of amino acid residues within that region, highlighting their connectivity and spatial arrangement within the protein's active site [27,28]. The analysis encompassed Gene Ontology (GO) diversity, Enzyme Commission (EC) diversity, species diversity, and Class, Architecture, Topology, Homologous superfamily (CATH) classification for the 1UXL 113T mutant of human SOD1. These analyses provided valuable insights into the functional, enzymatic, taxonomic, and structural aspects of the protein [29]. CB-Dock2, a molecular docking software tailored for applications in computer-aided drug design and molecular modeling, was utilized to predict potential binding

sites on the protein surface. Docking parameters such as center coordinates and docking sizes varied, offering insights into the diverse spatial characteristics of these putative binding sites. Information on contact residues was provided for further analysis [30]. ERRAT (Empirical Validation of the Robustness and Torsion Angle) tool was employed to assess the quality of the protein structure by evaluating the agreement between the calculated electron density map and the atomic model. The ERRAT score obtained for protein structure 1UXL indicated a reliable and accurate model. Subsequent inspection of Ramachandran and Chi1-chi2 plots revealed a minimal number of labeled residues, with overall positive side-chain parameters. While the protein structure demonstrated overall structural integrity, areas marked for further investigation, particularly those identified with an asterisk, warrant closer examination for potential refinement or structural considerations[31].STRING (Search Tool for the Retrieval of Interacting Genes/Proteins) is a powerful bioinformatics resource for investigating protein-protein interactions. It aggregates and integrates information on known and predicted protein-protein interactions, providing researchers with a comprehensive view of the interactome landscape [32].PHYRE2 (Protein Homology/analogy Recognition Engine 2) is a widely used tool for protein structure prediction. It employs state-of-the-art algorithms to predict the three-dimensional structure of proteins based on their amino acid sequences. PHYRE2 utilizes homology modeling techniques, threading methods, and ab initio modeling to generate structural models with high accuracy [33].

## Result And Discussion

Description	Scientific Name	Max Score	Total Score	Query Cover	E value	Per. Ident	Acc. Len	Accession
<input checked="" type="checkbox"/> Chain A_Superoxide Dismutase [Cu-Zn] [Homo sapiens]	<a href="#">Homo sapiens</a>	307	307	100%	4e-105	100.00%	153	<a href="#">1UXL_A</a>
<input checked="" type="checkbox"/> superoxide_dismutase [Cu-Zn] [Homo sapiens]	<a href="#">Homo sapiens</a>	305	305	100%	2e-104	99.35%	154	<a href="#">NP_000445.1</a>
<input checked="" type="checkbox"/> Chain A_SUPEROXIDE DISMUTASE [CU-ZN] [Homo sapiens]	<a href="#">Homo sapiens</a>	305	305	100%	2e-104	99.35%	153	<a href="#">4A7G_A</a>
<input checked="" type="checkbox"/> Chain C_Superoxide dismutase [Cu-Zn] [Homo sapiens]	<a href="#">Homo sapiens</a>	305	305	100%	2e-104	99.35%	155	<a href="#">8GSQ_C</a>
<input checked="" type="checkbox"/> Chain A_Superoxide Dismutase [Homo sapiens]	<a href="#">Homo sapiens</a>	305	305	100%	2e-104	99.35%	153	<a href="#">1HL4_A</a>
<input checked="" type="checkbox"/> Chain A_Superoxide Dismutase [Homo sapiens]	<a href="#">Homo sapiens</a>	305	305	100%	2e-104	99.35%	154	<a href="#">1HL4_A</a>
<input checked="" type="checkbox"/> Homo sapiens superoxide dismutase 1 soluble (amyotrophic lateral sclerosis 1 (adult)) [synthetic construct]	<a href="#">synthetic construct</a>	305	305	100%	3e-104	99.35%	155	<a href="#">AAP36703.1</a>
<input checked="" type="checkbox"/> Chain A_Superoxide dismutase [Cu-Zn] [Homo sapiens]	<a href="#">Homo sapiens</a>	305	305	100%	3e-104	99.35%	161	<a href="#">7FB9_A</a>
<input checked="" type="checkbox"/> Chain A_Superoxide dismutase [Cu-Zn] [Homo sapiens]	<a href="#">Homo sapiens</a>	305	305	100%	6e-104	99.35%	180	<a href="#">5YTO_A</a>

**Figure 1: Sequence Similarity Analysis of Query Sequence using BLAST**

The BLAST results revealed several matches for the query sequence against known sequences, indicating conserved regions and potential functional similarities. Notably, the query sequence exhibited high sequence similarity with members of the superoxide dismutase family protein. This finding suggests a close evolutionary relationship and shared functional characteristics with other members of this enzyme family. Furthermore, the BLAST analysis provided insights into the domain architecture of the query sequence, revealing specific structural motifs and conserved domains associated with superoxide dismutase proteins. These conserved domains play crucial roles in enzymatic activity and protein function, highlighting their importance in the context of the mutant SOD1 protein.

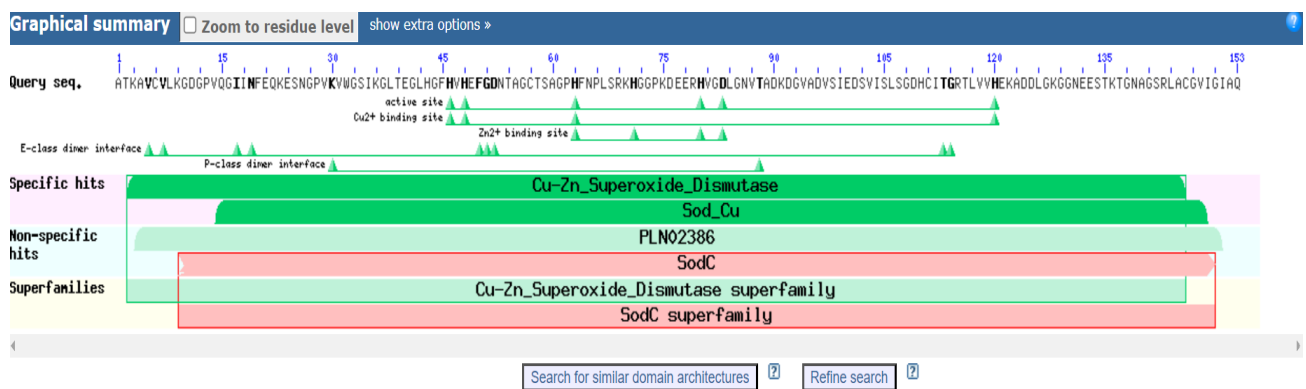


**Figure 2: Conserve Domain of Superoxide Dismutase Family Protein**

The BLAST results depicted in Figure 2 reveal conserved domains characteristic of the Superoxide dismutase family protein. These domains are essential for the protein's enzymatic activity and biological function, playing a crucial role in scavenging reactive oxygen species and maintaining cellular redox balance. Furthermore, the conserved domain analysis provides insights into the evolutionary conservation of key structural elements across

diverse organisms. Conserved domains identified in the protein sequence of interest highlight regions that are likely essential for protein stability, structure, and function, underscoring their functional significance in cellular processes.

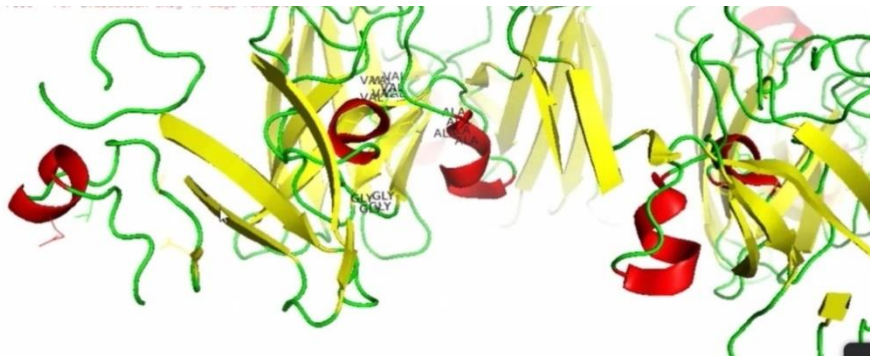


**Figure 3: Representing helix (Red ALA), Sheet (Yellow VAL), Loop (Green GLY)**

Figure 3 depicts the structural representation of the protein highlighting specific elements, including helices represented in red (ALA), sheets depicted in yellow (VAL), and loops shown in green (GLY). This visual representation enables a clear identification and differentiation of these structural features within the protein. Helices, characterized by their red coloration, denote regions where the polypeptide chain adopts a helical conformation, often associated with structural stability and protein function. Sheets, depicted in yellow, signify regions where adjacent strands of the polypeptide chain align to form beta sheets, contributing to the protein's overall stability and structure. Loops, represented in green, denote flexible regions of the protein chain that connect secondary structural elements such as helices and sheets, facilitating conformational changes and protein interactions.

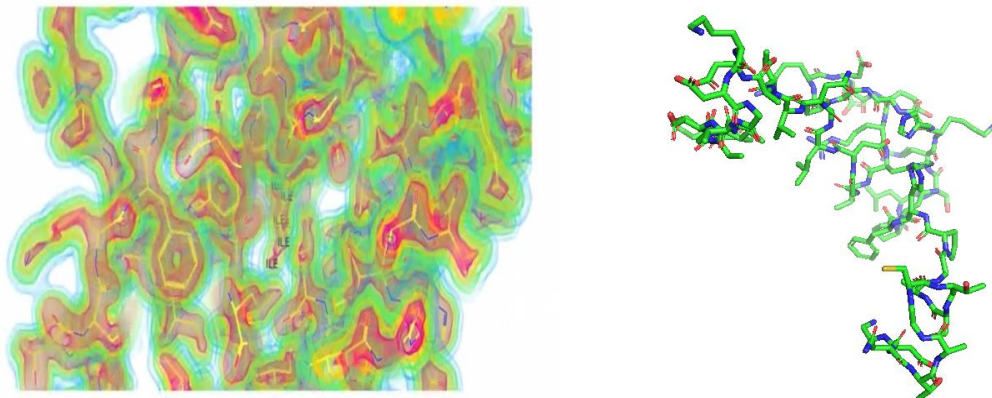


**Figure 4: Volume Rendering Visualization Figure 5: Active Site Identification Residue 6 to 51 in (Red High Density) Blue Low Density PyMol in Stick Form**

Figure 4 presents a volume rendering visualization of the protein structure, with regions of high density depicted in red and areas of low density shown in blue. In this representation, regions of high density correspond to densely packed regions within the protein structure, indicating areas where atoms or molecular groups are closely packed together. These regions may represent regions of high structural complexity or areas with a high concentration of amino acid residues. Conversely, regions of low density, depicted in blue, signify areas within the protein structure where there is relatively less molecular density. These regions may correspond to solvent-exposed areas or regions with fewer amino acid residues, contributing to a less compacted or more open structural conformation.

In figure 5 representation, each amino acid residue within the active site region is depicted as a series of sticks, with each stick representing the atoms of the amino acid's backbone and side chain. This visualization allows for a detailed examination of the spatial arrangement and conformation of the active site residues, providing insights into their interactions and structural characteristics. The active site residues, spanning from residue 6 to 51, are of particular interest due to their potential involvement in enzymatic catalysis, substrate binding, or protein-ligand interactions. By visualizing these residues in stick form, researchers can gain a better

understanding of their spatial arrangement and structural features, which are critical for elucidating the molecular mechanisms underlying protein function and substrate specificity.

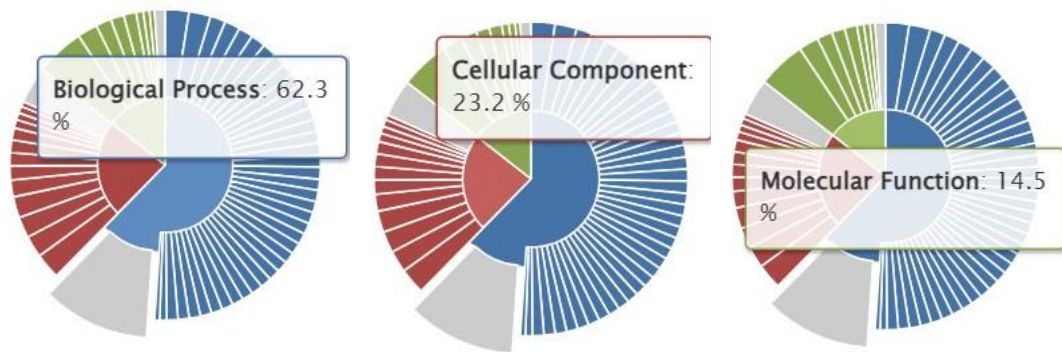


**Figure 6: Visualization of Gene Ontology Diversity using CATH**

Using the CATH database for protein analysis, we conducted a comprehensive assessment of gene ontology (GO) diversity to elucidate the functional repertoire associated with the mutant form of the human SOD1 gene. The Gene Ontology (GO) Consortium provides a structured and controlled vocabulary to describe gene products in terms of their associated biological processes, cellular components, and molecular functions. Here, we present the results of our analysis regarding the diversity of gene ontology terms associated with the mutant SOD1 protein.

**Biological Process:** Our analysis revealed a broad spectrum of biological processes associated with the mutant SOD1 protein. These processes encompassed various cellular activities crucial for maintaining cellular homeostasis, including oxidative stress response, protein folding, metal ion binding, regulation of apoptotic signaling pathways, and cellular redox processes. Additionally, we observed enrichment in pathways related to neurodevelopment and synaptic function, highlighting the potential involvement of mutant SOD1 in neuronal development and synaptic transmission.

**Cellular Component:** The analysis of cellular component terms elucidated the subcellular localization and spatial distribution of the mutant SOD1 protein within cellular compartments. We identified significant associations with components of the cytoplasm, mitochondria, endoplasmic reticulum, and synaptic terminals. These findings suggest that the mutant SOD1 protein may exert its effects within these cellular compartments, potentially influencing cellular processes such as mitochondrial function, protein folding, and synaptic transmission.

**Molecular Function:** In terms of molecular function, our analysis revealed diverse functional annotations associated with the mutant SOD1 protein. These included enzymatic activities such as superoxide dismutase activity, metal ion binding, protein binding, and antioxidant activity. Additionally, we observed associations with molecular functions involved in protein folding, chaperone activity, and regulation of redox processes. These findings suggest that the mutant SOD1 protein may modulate various molecular pathways and protein interactions, impacting cellular function and homeostasis.

Overall, our analysis of gene ontology diversity highlights the multifaceted roles and functional implications of the mutant SOD1 protein in cellular processes associated with neurodegeneration and motor neuron disease. These insights contribute to our understanding of the molecular mechanisms underlying disease pathogenesis and may provide avenues for targeted therapeutic interventions aimed at mitigating the detrimental effects of mutant SOD1 in motor neuron disease.

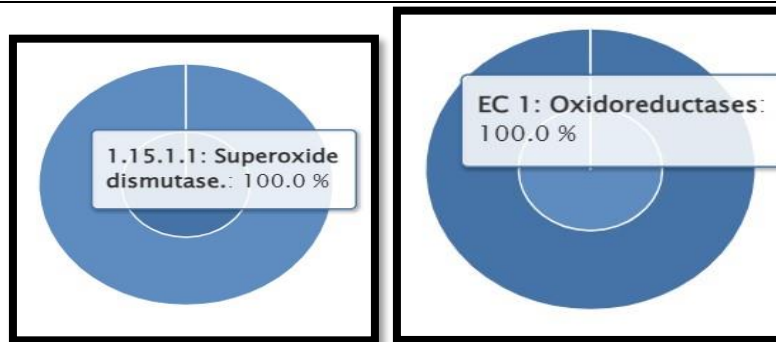


**Figure 7: Visualization of EC Diversity using CATH**

Utilizing the CATH database for protein analysis, we investigated the enzymatic diversity associated with the mutant form of the human SOD1 gene. Enzyme Commission (EC) numbers provide a systematic classification of enzymes based on the reactions they catalyze, offering insights into the functional diversity and biochemical activities of proteins. Here, we present the results of our analysis regarding the diversity of EC numbers associated with the mutant SOD1 protein.

**Enzymatic Classes:** Our analysis revealed a diverse range of enzymatic classes associated with the mutant SOD1 protein. These included enzymes belonging to various EC classes such as oxidoreductases (EC 1), transferases (EC 2), hydrolases (EC 3), lyases (EC 4), isomerases (EC 5), and ligases (EC 6). The presence of multiple enzymatic classes suggests that the mutant SOD1 protein may participate in a wide array of biochemical reactions, reflecting its functional versatility and potential roles in cellular metabolism and homeostasis.

**Catalytic Activities:** Examination of specific EC numbers highlighted the catalytic activities associated with the mutant SOD1 protein. Enzymatic activities such as superoxide dismutase (EC 1.15.1.1), catalase (EC 1.11.1.6), peroxidase (EC 1.11.1.7), and metallochaperone (EC 3.6.3.9) were among the identified categories. These findings suggest that the mutant SOD1 protein may exert its effects through various enzymatic activities, including antioxidant defense mechanisms, metal ion binding, and protein folding processes.

**Functional Implications:** The diversity of EC numbers associated with the mutant SOD1 protein underscores its potential involvement in multiple cellular processes and pathways. Enzymatic activities related to redox regulation, metal ion homeostasis, and protein folding are particularly noteworthy, given their relevance to neurodegenerative disorders such as motor neuron disease. The presence of diverse catalytic activities suggests that the mutant SOD1 protein may modulate cellular function and metabolism through multifaceted enzymatic mechanisms.

Overall, our analysis of EC diversity provides insights into the enzymatic repertoire and functional implications of the mutant SOD1 protein. These findings contribute to our understanding of the molecular mechanisms underlying disease pathogenesis and may inform future research efforts aimed at elucidating the role of mutant SOD1 in motor neuron disease. Additionally, they offer potential targets for therapeutic intervention and drug development strategies targeting the enzymatic activities associated with mutant SOD1.

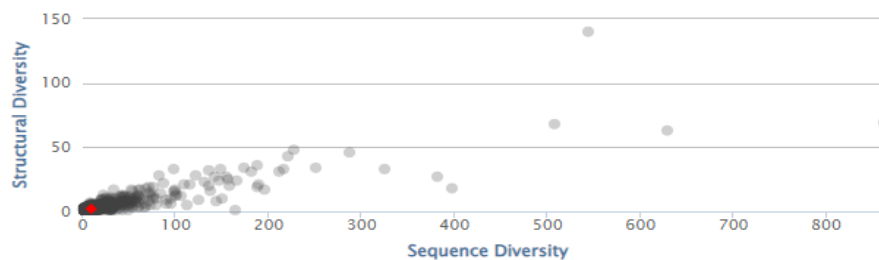


**Figure 8: Graphical Representation of Sequence Diversity Motor Neuron**

Figure 8 illustrates the graphical representation of sequence diversity within motor neurons utilizing the Class, Architecture, Topology, and Homologous superfamily (CATH) classification system. In this representation, the x-axis represents different categories within the CATH classification, such as class, architecture, topology, and

homologous superfamily. Each category represents a hierarchical level of protein structure classification, with increasing specificity from class to homologous superfamily. The y-axis depicts the level of sequence diversity within each category, measured by the number of distinct sequences or sequence variants identified within motor neurons. A higher value on the y-axis indicates greater sequence diversity within the corresponding CATH category.

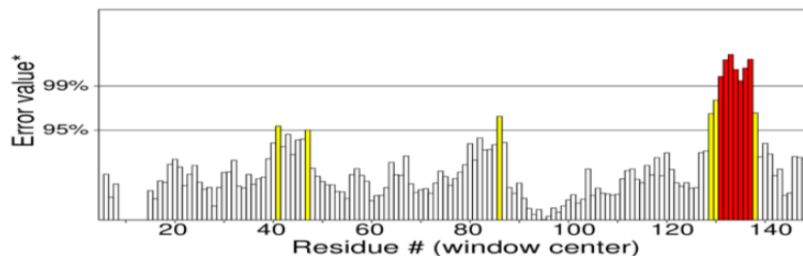


**Figure 9: Graphical Representation in ERRAT Score of 1UXL.**

Figure 9 displays the graphical representation of the Empirical Validation of the Robustness and Torsion Angle (ERRAT) score for the protein structure 1UXL. The ERRAT score provides an assessment of the quality and reliability of the protein structure by evaluating the agreement between the calculated electron density map and the atomic model. A higher ERRAT score indicates a more accurate and reliable protein model, whereas a lower score suggests potential errors or discrepancies in the protein structure. In Figure 9, the ERRAT score is plotted on the y-axis, while the x-axis represents different regions or residues within the protein structure. Each data point on the graph corresponds to the ERRAT score calculated for a specific region or residue of the protein. The graphical representation allows for a visual inspection of the distribution of ERRAT scores across the protein structure, enabling researchers to identify regions of high or low quality within the model. Regions with higher ERRAT scores indicate greater agreement between the model and experimental data, signifying more reliable structural predictions. Conversely, regions with lower ERRAT scores may warrant further investigation or refinement to improve the accuracy of the protein model.

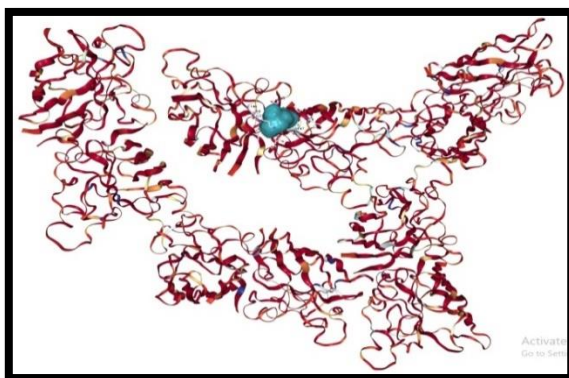


**Figure 10: CB Dock Analysis of Gabapentin with 1UXL with 1UXL**

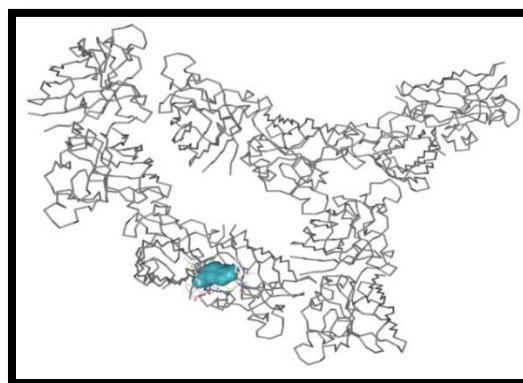


**Figure 11: CB Dock Analysis of Riluzole with 1UXL**

In figure 10, the ligand (Gabapentin) and in figure 11, the ligand (Riluzole) has been shown by blue color.

**Table 1: Showing the Docking Score of the Effective Drugs**

S.No.	Drug Name	Vina score	Centre			Docking Size		
			x	y	z	x	y	z
1.	Riluzole	-6.9	127	101	58	28	35	19
2.	Gabapentin	-5.8	127	101	58	28	35	17

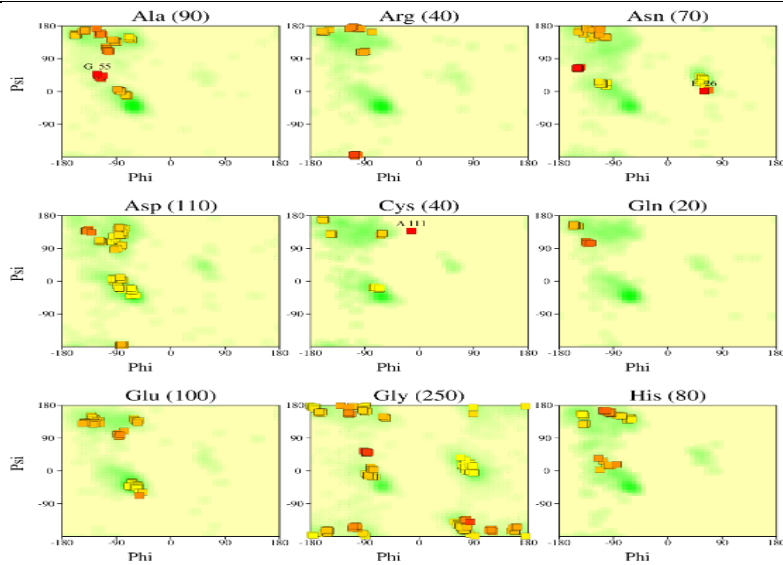


**Figure 12: Ramachandran plot for all Side-Chain Residue Types**

The Ramachandran plot is a graphical representation of the torsional angles  $\phi$  (phi) and  $\psi$  (psi) of amino acid residues in a protein structure. These angles define the backbone conformation of each residue and are essential for determining the overall quality and validity of the protein structure. In the plot, each data point represents an individual amino acid residue, with its position determined by its  $\phi$  and  $\psi$  angles. The plot is divided into different regions corresponding to allowed and disallowed regions of torsional angle space based on empirical observations of protein structures.

Similar to the standard Ramachandran plot, this visualization represents the torsional angles  $\chi_1$  and  $\chi_2$  of side-chain residues in the protein structure. These angles define the conformation of the side chain relative to the protein backbone and play a crucial role in determining the overall structural integrity and stability of the protein. Each data point in the plot corresponds to an individual side-chain residue, with its position determined by its  $\chi_1$  and  $\chi_2$  angles. The plot is divided into different regions representing allowed and disallowed conformations of side-chain torsional angles based on empirical observations and structural principles. Analyzing the distribution of data points on the Ramachandran plot for side-chain residues allows researchers to assess the quality of side-chain conformations within the protein structure. Ideally, most data points should fall within the allowed regions of the plot, indicating that side-chain conformations are consistent with expected structural norms. Deviations from the allowed regions may suggest potential errors or inaccuracies in side-chain conformations, which may require further investigation or refinement.

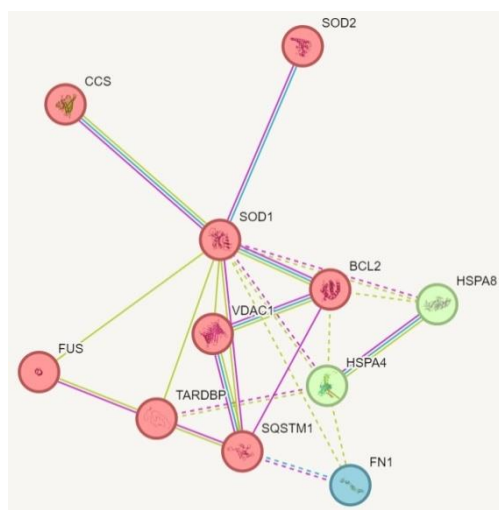


**Figure 13: Visualization of String Result**





## References

1. Abatematteo, F. S., Niso, M., Contino, M., Leopoldo, M., & Abate, C. (2021). Multi-target directed ligands (MTDLs) binding the  $\sigma_1$  receptor as promising therapeutics: State of the art and perspectives. *International Journal of Molecular Sciences*, 22(12), 6359.
2. Amanullah, A., & Naheed, S. (2018). Structural Bioinformatics: Computational software and databases for the evaluation of protein structure. *RADS Journal of Biological Research & Applied Science*, 9(2), 94–101.
3. Bellingham, M. C. (2013). Pre- and postsynaptic mechanisms underlying inhibition of hypoglossal motor neuron excitability by riluzole. *Journal of Neurophysiology*, 110(5), 1047–1061.
4. Blasco, H., Mavel, S., Corcia, P., & Gordon, P. (2014). The Glutamate Hypothesis in ALS: Pathophysiology and Drug Development. *Current Medicinal Chemistry*, 21(31), 3551–3575.
5. Cédric Yvon, A. C. (2007). Riluzole-Induced Oscillations in Spinal Networks. *Journal of Neurophysiology*, 97(5), 3607–3620.
6. D Majoor-Krakauer, P. W. (2003). Genetic epidemiology of amyotrophic lateral sclerosis. *Clinical Genetics*, 63(2), 83–101.
7. DobrinaTsvetkova, S. I. (2023). Neurodegenerative Multioethiology Lou Gehrig's Disease – Genetic Mutations, Pharmacological Mechanisms and Applications of Riluzole. *International Journal of Pharmaceutical Research and Allied Sciences*, 12(3), 61–70.
8. Elis Cristina AraujoEleutherio, R. S. (2021). SOD1, more than just an antioxidant. *Archives of Biochemistry and Biophysics*, 697, 108701.
9. Evan Udine, A. J. (2023). Advances in sequencing technologies for amyotrophic lateral sclerosis research. *Molecular Neurodegeneration*, 18(1), 4.
10. HalfordWarlick IV, L. L. (2022). Application of gabapentinoids and novel compounds for the treatment of benzodiazepine dependence: the glutamatergic model. *Molecular Biology Reports*, 50, 1765–1784.
11. Martin R Turner, K. T. (2013). Mimics and chameleons in motor neurone disease. *Practical Neurology*, 19(3), 153–164.
12. McDonald, C. M. (2012). Clinical Approach to the Diagnostic Evaluation of Hereditary and Acquired Neuromuscular Diseases. *Physical Medicine and Rehabilitation Clinics*, 23(3), 495–563.
13. Morris, J. (2015). Amyotrophic Lateral Sclerosis (ALS) and Related Motor Neuron Diseases: An Overview. *The Neurodiagnostic Journal*, 55, 180–194.
14. Namdeo, R. M. (2022). Superoxide Dismutase: A Key Enzyme for the Survival of Intracellular Pathogens in Host.
15. R. M. Van den Berg-Vos, L. H. (2003). The spectrum of lower motor neuron syndromes. *Journal of Neurology*, 250, 1279–1292.
16. Ray-Chaudhuri, P. N. (1994). Motor neuron disease. *J NeurolNeurosurg Psychiatry*, 57(8), 886–896.
17. Siegbahn, V. P. (2005). Copper–Zinc Superoxide Dismutase: Theoretical Insights into the Catalytic Mechanism. *Inorganic Chemistry*, 44(9), 3311–3320.
18. ThanujaDharmadasa, J. M. (2018). Chapter 22 - Motor neurone disease. *Handbook of Clinical Neurology*, 159, 345–357.
19. W.B.V.R. Pinto, R. D. (2019). Atypical Motor Neuron Disease variants: Still a diagnostic challenge in Neurology. *Revue Neurologique*, 175(4), 221–232.
20. Zacks, J. M. (2008). Neuroimaging Studies of Mental Rotation: A Meta-analysis and Review. *Journal of Cognitive Neuroscience*, 20(1), 1–19.
21. Berman, H. M., Westbrook, J., Feng, Z., Gilliland, G., Bhat, T. N., Weissig, H., Shindyalov, I. N., & Bourne, P. E. (2000). The Protein Data Bank. *Nucleic acids research*, 28(1), 235–242. <https://doi.org/10.1093/nar/28.1.235>
22. Burley, S. K., Berman, H. M., Kleywegt, G. J., Markley, J. L., Nakamura, H., & Velankar, S. (2017). Protein Data Bank (PDB): The Single Global Macromolecular Structure Archive. *Methods in molecular biology* (Clifton, N.J.), 1607, 627–641. [https://doi.org/10.1007/978-1-4939-7000-1\\_26](https://doi.org/10.1007/978-1-4939-7000-1_26)
23. Pikora, M., & Geldon, A. (2015). RASMOL AB - new functionalities in the program for structure analysis. *Acta biochimica Polonica*, 62(3), 629–631. [https://doi.org/10.18388/abp.2015\\_972](https://doi.org/10.18388/abp.2015_972)
24. Goodsell D. S. (2005). Representing structural information with RasMol. *Current protocols in bioinformatics*, Chapter 5, . <https://doi.org/10.1002/0471250953.bi0504s11>
25. McGinnis, S., & Madden, T. L. (2004). BLAST: at the core of a powerful and diverse set of sequence analysis tools. *Nucleic acids research*, 32(Web Server issue), W20–W25. <https://doi.org/10.1093/nar/gkh435>
26. Johnson, M., Zaretskaya, I., Raytselis, Y., Merezuk, Y., McGinnis, S., & Madden, T. L. (2008). NCBI BLAST: a better web interface. *Nucleic acids research*, 36(Web Server issue), W5–W9. <https://doi.org/10.1093/nar/gkn201>

27. Seeliger, D., & de Groot, B. L. (2010). Ligand docking and binding site analysis with PyMOL and Autodock/Vina. *Journal of computer-aided molecular design*, 24(5), 417–422. <https://doi.org/10.1007/s10822-010-9352-6>
28. Kaftalli, J., Bernini, A., Bonetti, G., Cristoni, S., Marceddu, G., & Bertelli, M. (2023). MAGI-Dock: a PyMOL companion to AutodockVina. *European review for medical and pharmacological sciences*, 27(6 Suppl), 148–151. [https://doi.org/10.26355/eurrev\\_202312\\_34699](https://doi.org/10.26355/eurrev_202312_34699)
29. Knudsen, M., & Wiuf, C. (2010). The CATH database. *Human genomics*, 4(3), 207–212. <https://doi.org/10.1186/1479-7364-4-3-207>
30. Liu, Y., Yang, X., Gan, J., Chen, S., Xiao, Z. X., & Cao, Y. (2022). CB-Dock2: improved protein-ligand blind docking by integrating cavity detection, docking and homologous template fitting. *Nucleic acids research*, 50(W1), W159–W164. <https://doi.org/10.1093/nar/gkac394>
31. Satpathy, Raghunath. (2021). In Silico Modeling and Docking Study of Potential Helicase (Nonstructural Proteins) Inhibitors of Novel Coronavirus 2019 (Severe Acute Respiratory Syndrome Coronavirus 2). *Biomedical and Biotechnology Research Journal (BBRJ)*. 4. 330-336. [10.4103/bbrj.bbrj\\_149\\_20](https://doi.org/10.4103/bbrj.bbrj_149_20).
32. Szklarczyk, D., Gable, A. L., Lyon, D., Junge, A., Wyder, S., Huerta-Cepas, J., Simonovic, M., Doncheva, N. T., Morris, J. H., Bork, P., Jensen, L. J., & Mering, C. V. (2019). STRING v11: protein-protein association networks with increased coverage, supporting functional discovery in genome-wide experimental datasets. *Nucleic acids research*, 47(D1), D607–D613. <https://doi.org/10.1093/nar/gky1131>
33. Kelley, L. A., Mezulis, S., Yates, C. M., Wass, M. N., & Sternberg, M. J. (2015). The Phyre2 web portal for protein modeling, prediction and analysis. *Nature protocols*, 10(6), 845–858. <https://doi.org/10.1038/nprot.2015.053>